DALTON
FULL PAPER

Structure and magnetic and electrochemical properties of (μ-aryloxo)-bis(μ-carboxylato)diruthenium(III) complexes

Yuji Mikata,[*,a] **Nao Takeshita,**[a] **Tomoko Miyazu,**[a] **Yuki Miyata,**[a] **Tomoaki Tanase,**[*,a] **Isamu Kinoshita,**[b] **Akio Ichimura,**[b] **Wasuke Mori,**[c] **Satoshi Takamizawa**[d] **and Shigenobu Yano**[*,a]

[a] *Department of Chemistry, Faculty of Science, Nara Women's University, Nara 630, Japan*
[b] *Department of Chemistry, Faculty of Science, Osaka City University, Sumiyoshi-ku, Osaka 558, Japan*
[c] *Department of Chemistry, Faculty of Science, Kanagawa University, Hiratsuka, Kanagawa 259-12, Japan*
[d] *Department of Chemistry, Faculty of Science, Osaka University, Toyonaka-shi, Osaka 550, Japan*

The dinuclear diruthenium complexes ligated by the (μ-aryloxo)bis(μ-carboxylato) system $M[Ru_2L(\mu\text{-}O_2CR)_2]$ (M = Na, R = Me **1**; M = Na, R = Ph **2**; M = K, R = Me **3**; M = K, R = Ph **4**; H_5L = 2-hydroxy-5-methyl-*m*-phenylenedimethylenedinitrilotetraacetic acid) were prepared by the reaction of $[RuCl_2(Me_2SO)_4]$ with L^{5-} and carboxylic acid. The structure of the benzoate-bridged complex **4**·0.5MeOH·0.5EtOH·4H$_2$O was elucidated by X-ray crystallography. The Ru···Ru distance was 3.416 Å (average for two crystallographically independent molecules), comparable to those of (μ-alkoxo)bis(μ-carboxylato)diruthenium complexes. The magnetic properties were analysed by a general isotropic exchange Hamiltonian $H = -2JS_1 \cdot S_2$ ($S_1 = S_2 = \frac{1}{2}$), yielding meaningfully large antiferromagnetic spin coupling constants ($-J$ = 728 and 649 cm^{-1} for **1** and **2**, respectively). The cyclic voltammogram of **4** in dmf demonstrated two reduction and one oxidation wave corresponding to the four redox states Ru^{II}_2, $Ru^{II}Ru^{III}$, Ru^{III}_2, $Ru^{III}Ru^{IV}$. The intervalence coupling constant K_C estimated from the potential gap between $Ru^{II}_2/Ru^{II}Ru^{III}$ and $Ru^{II}Ru^{III}/Ru^{III}_2$ indicated that the introduction of the μ-aryloxo bridge stabilizes the $Ru^{II}Ru^{III}$ mixed-valence species.

Oxo-, hydroxo- and alkoxo-bridged diiron complexes are of considerable interest as models for hemerythrin, ribonucleotide reductase, and methane monooxygenase.[1–3] The parallel chemistry by utilizing ruthenium centres is also a prospective subject since it allows a wide variety of oxidation states,[4–7] which is useful to establish new physical and chemical properties. Recently, we have reported the (μ-alkoxo)bis(μ-carboxylato)diruthenium(III) complexes, $[Ru_2(dhpta)(\mu\text{-}O_2CR)_2]^-$ (H_5dhpta = 2-hydroxytrimethylenedinitrilotetraacetic acid), which involve a related system to non-heme diiron active centres and indicate that their physical properties could be tuned by varying the monoatom-bridging group.[8,9] We report herein the synthesis and characterization of (μ-aryloxo)bis(μ-carboxylato)diruthenium(III) complexes, $[Ru_2L(\mu\text{-}O_2CR)_2]^-$ (H_5L = 2-hydroxy-5-methyl-*m*-phenylenedimethylenedinitrilotetraacetic acid), in which the aryloxo-bridge significantly influences their electrochemical and magnetic properties.

Experimental

Instrumental

Proton NMR spectra were recorded on a Varian GEMINI 2000 and a JEOL GX-400 spectrometer at 300 and 400 MHz, respectively, in D$_2$O, electronic absorption spectra on a JASCO V-570 spectrophotometer. Cyclic voltammograms were obtained using a BASCV-50W voltammetric analyser using a three-electrode system, *i.e.* glassy carbon (working electrode), platinum wire (counter electrode) and Ag–AgPF$_6$ reference electrode. Magnetic susceptibility data were recorded by the Faraday method over a temperature range 78–300 K with a Cahn 1000 RH electrobalance; values at room temperature were also measured by the Gouy method. The diamagnetism of the complexes was corrected from Pascal's constants. The temperature dependence of the molar susceptibility was analysed by a similar method to that reported[9] based on a general isotropic exchange Hamiltonian $H = -2JS_1 \cdot S_2$ ($S_1 = S_2 = \frac{1}{2}$), using the van Vleck equation (1), where N = Avogadro's number, β = Bohr magneton and k = Boltzmann's constant.

$$\chi_m = \left(\frac{N_g{}^2\beta^2}{3kT}\right)\frac{1}{1 + (1/3)\exp(-2J/kT)} + N_\alpha \qquad (1)$$

General method for preparation of M[Ru$_2$L(μ-O$_2$CR)$_2$] (M = Na, R = Me 1; M = Na, R = Ph 2; M = K, R = Me 3; M = K, R = Ph 4)

To an aqueous solution (pH 5) of $M_nH_{5-n}L$ (M = Na or K, n = 1 or 2)[10] (0.17 g, 0.50 mmol), $[RuCl_2(Me_2SO)_4]$ (0.49 g, 1.0 mmol) was added and the mixture heated to 90–95 °C. Keeping the pH at 5 by addition of aqueous NaOH or KOH, the reaction mixture was stirred for 20–60 min. Then, an aqueous solution (pH 5) of the carboxylate (1.0 mmol) was added and stirred for 20 h with heating at 90–95 °C. The progress of the reaction was monitored by UV/VIS spectra around 500 nm. The resulting dark red solution was concentrated *in vacuo* and purified by gel permeation chromatography (Sephadex G-15, eluted by water). Recrystallisation of the crude product from water–ethanol gave dark violet crystals in 3–15% yield.

Na[Ru$_2$L(μ-O$_2$CMe)$_2$]·6H$_2$O (1·6H$_2$O). Yield: 13 mg (0.015 mmol, 3%). ^{1}H NMR in D$_2$O (300 MHz): δ −7.93 (d, br, 2 H), −6.50 (d, br, 2 H), −3.68 (d, br, 2 H), −3.36 (d, br, 2 H), −2.90 (d, br, 2 H), 0.50 (d, br, 2 H), 3.27 (s, 6 H), 5.91 (s, 3 H) and 8.87 (s, 2 H) (Found: C, 29.47; H, 3.87; N, 3.23. Calc. for **1**·6H$_2$O: C, 29.79; H, 4.41; N, 3.31%). λ_{max}/nm (dmf) (ε/M^{-1} cm^{-1}) 479 (1.42 × 10^3) and 386 (1.66 × 10^3).

Na[Ru$_2$L(μ-O$_2$Ph)$_2$]·3.5H$_2$O (2·3.5H$_2$O). Yield: 24 mg (0.026 mmol, 5%). ^{1}H NMR in D$_2$O (300 MHz): δ −7.81 (d, br, 2 H), −6.48 (d, br, 2 H), −3.58 (s, br, 4 H), −3.47 (s, br, 2 H), 0.43 (d, br, 2 H), 5.68 (s, 3 H), 7.24 (s, 10 H) and 8.82 (s, 2 H) (Found: C, 40.41; H, 3.68; N, 3.14. Calc. for **2**·3.5H_2O: C, 40.87; H, 4.16; N, 2.89%). λ_{max}/nm (dmf) (ε/M^{-1} cm^{-1}) 480 (1.54×10^3) and 382 (2.30×10^3).

K[Ru_2L(μ-O_2CMe)$_2$]·7H_2O (3·7H_2O). Yield: 31 mg (0.035 mmol, 7%). ^{1}H NMR in D_2O (300 MHz): δ −7.96 (d, br, 2 H), −6.55 (d, br, 2 H), −3.72 (d, br, 2 H), −3.40 (d, br, 2 H), −2.95 (d, br, 2 H), 0.46 (d, br, 2 H), 3.23 (s, 6 H), 5.88 (s, 3 H) and 8.85 (s, 2 H) (Found: C, 28.71; H, 3.81; N, 3.22. Calc. for **3**·7H_2O: C, 28.70; H, 4.24; N, 3.19%). λ_{max}/nm (dmf) (ε/M^{-1} cm^{-1}) 483 (1.51×10^3) and 386 (1.79×10^3).

K[Ru_2L(μ-O_2CPh)$_2$]·5H_2O (4·5H_2O). Yield: 73 mg (0.076 mmol, 15%). ^{1}H NMR in D_2O (300 MHz): δ −7.84 (s, br, 2 H), −6.48 (d, br, 2 H), −3.60 (s, br, 4 H), −3.44 (s, br, 2 H), 0.42 (d, br, 2 H), 5.68 (s, 3 H), 7.23 (s, 10 H) and 8.83 (s, 2 H) (Found: C, 38.61; H, 3.86; N, 2.83. Calc. for **4**·5H_2O: C, 38.51; H, 3.86; N, 2.90%). λ_{max}/nm (dmf) (ε/M^{-1} cm^{-1}) 484 (1.94×10^3) and 382 (2.92×10^3).

X-Ray crystallography

A violet crystal of complex **4**·0.5MeOH·0.5EtOH·4H_2O grown from a methanol–ethanol–water mixed solvent was mounted on the end of a glass fibre with Paraton N oil at −137 °C. Crystal data and experimental conditions are given in Table 1. Data were collected on a Rigaku AFC7R diffractometer with graphite-monochromated Mo-Kα radiation using the ω–2θ scanning technique. The data were corrected for Lorentz-polarization effects and for absorption effects by the ψ-scan method. The intensities of three representative reflections were measured every 150 and showed no systematic decrease in intensity. The structure was solved by direct methods (SIR 92),[11] and refined with full-matrix least-squares techniques. Hydrogen atoms were calculated at positions with C–H 0.95 Å and not refined. The final refinement was carried out with anisotropic thermal parameters for all non-hydrogen atoms, minimizing $\Sigma w(|F_o| - |F_c|)^2$ using standard neutral atom dispersion factors and anomalous dispersion corrections.[12,13] All calculations were performed using the TEXSAN crystallographic package.[14] Perspective drawings were drawn by using ORTEP.[15]

CCDC reference number 186/982.

Results and Discussion

Compounds M[Ru_2L(μ-O_2CR)$_2$] (M = Na, R = Me **1**; M = Na, R = Ph **2**; M = K, R = Me **3**; M = K, R = Ph **4**) were synthesized in 3–15% yield from [$RuCl_2(Me_2SO)_4$] by a procedure similar to that for (μ-alkoxo)bis(μ-carboxylato)diruthenium complexes[8,9] using H_5L[10] in place of H_5dhpta. Their IR and electronic absorption spectra were similar to those of (μ-alkoxo)-diruthenium complexes. In the IR spectra, stretching vibrations around 1645–1500 and 1470–1325 cm^{-1}, assigned to $\nu_{asym}(CO_2)$ and $\nu_{sym}(CO_2)$, respectively, were detected, and in the visible spectra λ_{max} around 400 and 500 nm were observed. These spectroscopic properties are similar to those of corresponding (μ-alkoxo)bis(μ-carboxylato)diruthenium derivatives.

The rather sharp ^{1}H NMR spectra of these complexes in D_2O indicated a strong antiferromagnetic interaction between two ruthenium centres at room temperature. Fig. 1 shows the 400 MHz ^{1}H NMR spectra of **1** and **2** together with the proton assignment derived from a two-dimensional experiment. The paramagnetic upfield shifts for the methylene protons of the carboxylate arms of L (δ −7.8 to −7.9 and −6.5) were larger than those observed in the corresponding (μ-alkoxo)-bis(μ-carboxylato)diruthenium complex, K[Ru_2(dhpta)(μ-O_2CMe)$_2$] **5** (δ −5.7 and −4.0). The spectra indicated the presence of one kind of carboxylate ligand, whereas that of **5** exhibited two non-equivalent ones. This indicates a different symmetrical structure of **3** from that of the alkoxo-bridged complex **5** having C_s symmetry.

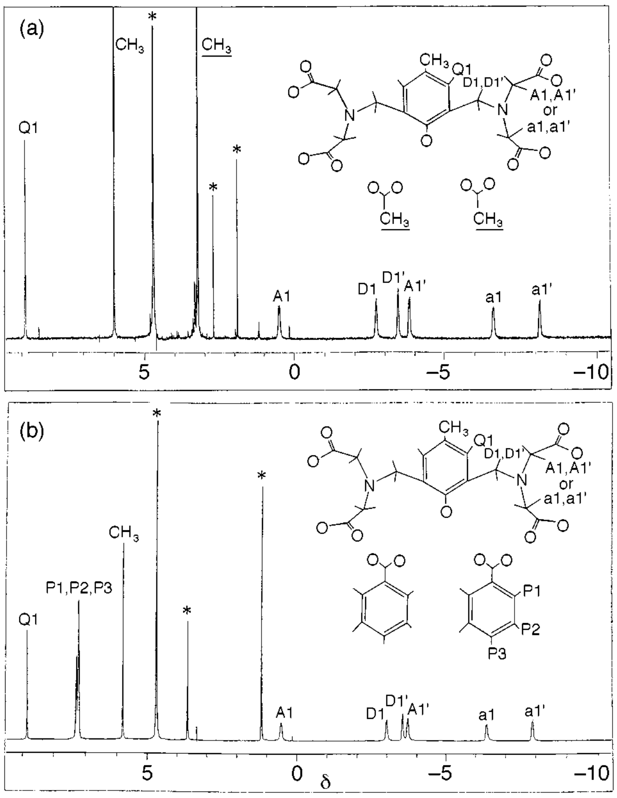

Fig. 1 400 MHz ^{1}H NMR spectra in D_2O and peak assignments of diruthenium complexes **1** (a) and **2** (b). Asterisks denote peaks due to solvents and impurities

A suitable single crystal of complex **4**·0.5MeOH·0.5EtOH·4H_2O obtained from a methanol–ethanol–water mixed solvent was subjected to X-ray crystallography. The experimental details are shown in Table 1. The asymmetric unit contains two crystallographically independent complex anions, their structures being almost identical and possessing a pseudo-C_2 axis along the aryloxo C–O bond. The complex anions were revealed to comprise a (μ-aryloxo)bis(μ-carboxylato)-diruthenium(III) centre ligated by L and two benzoate ligands (Fig. 2, only one complex anion is illustrated). Selected bond distances and angles are listed in Table 2. The average Ru–Ru interatomic distance is 3.416 Å, which is comparable to those of (μ-alkoxo)bis(μ-carboxylato)diruthenium complexes (3.420–3.433 Å).[8,9] The most conspicuous feature is in the planar structure of the μ-phenolate oxygen atoms, the sum of the three bond angles being 359.9° (average), in contrast with that of the μ-alkoxo oxygen atoms in **5** which deviate considerably from planarity (average 351°). The phenyl ring delocalizes the lone-pair electron density of the aryloxo oxygen and increases the p character of its valence orbitals, as evidenced by the longer Ru–O distances (average 1.985 Å) and the smaller Ru–O–Ru angles (average 118.8°) than those observed in the μ-alkoxo complex **5** (average Ru–O 1.947 Å, average Ru–O–Ru 122.9°). These slight but meaningful structural changes should be responsible for the magnetic and electrochemical properties although the Ru···Ru distance is unchanged in comparison with **5** (see below).

Complexes **1** and **2** are paramagnetic at room temperature as is shown by the isotropically shifted ^{1}H NMR spectra. The temperature-dependent magnetic susceptibilities of **1** and **2** were measured and analysed by a general isotropic exchange Hamiltonian, $H = -2JS_1 \cdot S_2$ ($S_1 = S_2 = \frac{1}{2}$), to generate an antiferromagnetic intramolecular spin coupling constant $-J$, Lande's g factor and temperature-independent paramagnetism (N_α). The results are presented in Fig. 3 and Table 3. The anti-

Table 1 Crystallographic and experimental data for complex **4**·0.5MeOH·0.5EtOH·4H$_2$O

Formula	$C_{32.5}H_{40}KN_2O_{18}Ru_2$
M	987.91
Crystal size/mm	0.45 × 0.30 × 0.20
Crystal system	Monoclinic
Space group	$P2_1/n$
a/Å	17.751(7)
b/Å	14.575(5)
c/Å	29.949(9)
β/°	100.25(3)
U/Å^3	7624(4)
Z	8
D_c/g cm^{-3}	1.72
Transmission factors	0.82–0.99
2θ Range/°	3–50
No. unique data	14 009
No. observed data	9588 [$I > 3\sigma(I)$]
No. variables	999
R[a]	0.050
R′[b]	0.057
Goodness of fit	1.90

[a] $\Sigma||F_o| - |F_c||/\Sigma|F_o|$. [b] $[\Sigma w(|F_o| - |F_c|)^2/\Sigma w|F_o|^2]^{\frac{1}{2}}$, $w = 1/\sigma^2(F_o)$.

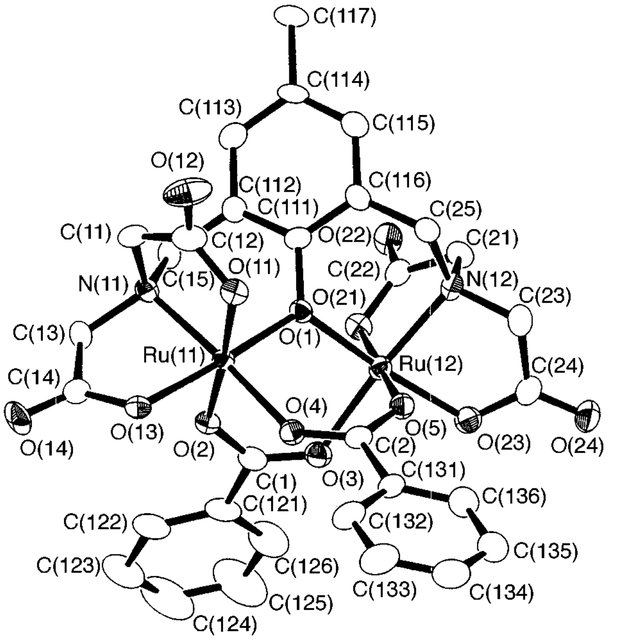

Fig. 2 An ORTEP drawing for one of the two independent complex anions of K[Ru$_2$L(μ-O$_2$CPh)$_2$] **4**

Table 2 Selected bond distances (Å) and angles (°) for complex **4**·0.5MeOH·0.5EtOH·4H$_2$O

Ru(11)···Ru(12)	3.439(1)	Ru(21)···Ru(22)	3.3921(9)
Ru(11)–O(1)	1.983(5)	Ru(21)–O(6)	1.985(5)
Ru(11)–O(2)	2.056(5)	Ru(21)–O(7)	2.077(5)
Ru(11)–O(4)	2.085(5)	Ru(21)–O(9)	2.042(5)
Ru(11)–O(11)	1.987(5)	Ru(21)–O(31)	1.999(5)
Ru(11)–O(13)	2.012(5)	Ru(21)–O(33)	2.017(5)
Ru(11)–N(11)	2.033(6)	Ru(21)–N(21)	2.034(6)
Ru(12)–O(1)	1.983(5)	Ru(22)–O(6)	1.987(5)
Ru(12)–O(3)	2.075(5)	Ru(22)–O(8)	2.046(5)
Ru(12)–O(5)	2.039(5)	Ru(22)–O(10)	2.083(6)
Ru(12)–O(21)	2.003(5)	Ru(22)–O(41)	1.989(6)
Ru(12)–O(23)	2.008(5)	Ru(22)–O(43)	2.009(5)
Ru(12)–N(12)	2.031(6)	Ru(22)–N(22)	2.031(7)
O(1)–Ru(11)–O(2)	88.8(2)	O(6)–Ru(21)–O(7)	94.5(2)
O(1)–Ru(11)–O(4)	93.2(2)	O(6)–Ru(21)–O(9)	87.9(2)
O(1)–Ru(11)–O(11)	90.7(2)	O(6)–Ru(21)–O(31)	89.3(2)
O(1)–Ru(11)–O(13)	173.5(2)	O(6)–Ru(21)–O(33)	172.9(2)
O(1)–Ru(11)–N(11)	94.4(2)	O(6)–Ru(21)–N(21)	95.1(2)
O(2)–Ru(11)–O(4)	91.9(2)	O(7)–Ru(21)–O(9)	93.6(2)
O(2)–Ru(11)–O(11)	175.7(2)	O(7)–Ru(21)–O(31)	90.2(2)
O(2)–Ru(11)–O(13)	86.2(2)	O(7)–Ru(21)–O(33)	89.7(2)
O(2)–Ru(11)–N(11)	91.4(2)	O(7)–Ru(21)–N(21)	169.0(2)
O(4)–Ru(11)–O(11)	92.4(2)	O(9)–Ru(21)–O(31)	175.4(2)
O(4)–Ru(11)–O(13)	91.3(2)	O(9)–Ru(21)–O(33)	86.1(2)
O(4)–Ru(11)–N(11)	171.8(2)	O(9)–Ru(21)–N(21)	91.9(2)
O(11)–Ru(11)–O(13)	93.8(2)	O(31)–Ru(21)–O(33)	96.4(2)
O(11)–Ru(11)–N(11)	84.4(2)	O(31)–Ru(21)–N(21)	84.7(2)
O(13)–Ru(11)–N(11)	81.5(2)	O(33)–Ru(21)–N(21)	81.2(2)
O(1)–Ru(12)–O(3)	94.4(2)	O(6)–Ru(22)–O(8)	87.7(2)
O(1)–Ru(12)–O(5)	89.7(2)	O(6)–Ru(22)–O(10)	95.1(2)
O(1)–Ru(12)–O(21)	89.4(2)	O(6)–Ru(22)–O(41)	90.4(2)
O(1)–Ru(12)–O(23)	173.2(2)	O(6)–Ru(22)–O(43)	175.1(2)
O(1)–Ru(12)–N(12)	94.7(2)	O(6)–Ru(22)–N(22)	94.8(2)
O(3)–Ru(12)–O(5)	91.0(2)	O(8)–Ru(22)–O(10)	93.3(2)
O(3)–Ru(12)–O(21)	89.8(2)	O(8)–Ru(22)–O(41)	176.4(2)
O(3)–Ru(12)–O(23)	90.3(2)	O(8)–Ru(22)–O(43)	88.3(2)
O(3)–Ru(12)–N(12)	169.0(2)	O(8)–Ru(22)–N(22)	92.8(2)
O(5)–Ru(12)–O(21)	178.8(2)	O(10)–Ru(22)–O(41)	90.0(2)
O(5)–Ru(12)–O(23)	85.3(2)	O(10)–Ru(22)–O(43)	88.0(2)
O(5)–Ru(12)–N(12)	95.1(2)	O(10)–Ru(22)–N(22)	168.6(2)
O(21)–Ru(12)–O(23)	95.6(2)	O(41)–Ru(22)–O(43)	93.4(2)
O(21)–Ru(12)–N(12)	84.3(2)	O(41)–Ru(22)–N(22)	84.2(2)
O(23)–Ru(12)–N(12)	81.2(2)	O(43)–Ru(22)–N(22)	82.6(2)
Ru(11)–O(1)–Ru(12)	120.3(2)	Ru(21)–O(6)–Ru(22)	117.3(2)
Ru(11)–O(1)–C(111)	121.2(4)	Ru(21)–O(6)–C(211)	120.8(4)
Ru(12)–O(1)–C(111)	118.3(4)	Ru(22)–O(6)–C(211)	121.8(4)

Estimated deviations are given in parentheses.

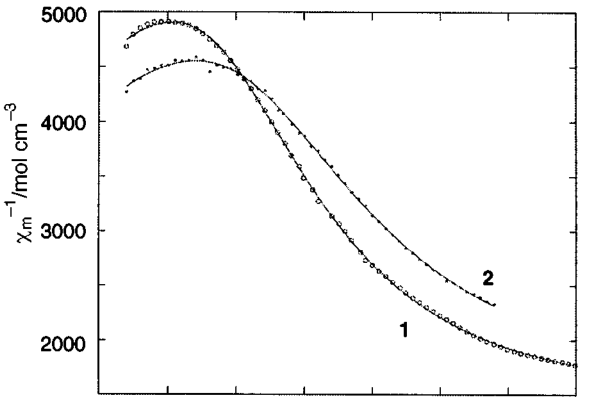

Fig. 3 Temperature dependence of the magnetic susceptibility data for diruthenium complexes **1** and **2**. The solid lines are best fits with equation (1)

ferromagnetic spin coupling constants for **1** and **2** are meaningfully larger than those for the dhpta complexes[9] in spite of similar interruthenium distances (3.416–3.433 Å). The stronger metal–metal antiferromagnetic interaction might be ascribable to an increasing overlap between d orbitals of Ru atoms and the p orbital of the phenolate oxygen atom on the basis of the crystal structure of **4**.

The electrochemical properties of complexes **1**–**4** were investigated by cyclic voltammetry in dmf solution with 0.1 M tetrabutylammonium hexafluorophosphate as supporting electrolyte. The potentials were referenced to a Ag–AgPF$_6$ electrode in MeCN. The cyclic voltammogram of **4** demonstrated two reduction and one oxidation waves at $E_{\frac{1}{2}} = -1.78$, -1.18 and 0.76 V, presumably corresponding to the respective one-electron redox processes of Ru^{II}Ru^{II}–Ru^{II}Ru^{III} ($E^1_{\frac{1}{2}}$), Ru^{II}Ru^{III}–Ru^{III}Ru^{III} ($E^2_{\frac{1}{2}}$) and Ru^{III}Ru^{III}–Ru^{III}Ru^{IV} ($E^3_{\frac{1}{2}}$) (Fig. 4, Table 4). The Ru$^{III}_2$ complexes of L undergo one-electron oxidation and reduction at more positive potentials than those of the dhpta complexes,[8,9] which is consistent with the poor electron donating ability of aryloxo compared with alkoxo groups. The reduction process Ru^{II}Ru^{II}–Ru^{II}Ru^{III} in L complexes, however, occurred at almost the same potential with dhpta complexes. The comproportionation constants (K_C) for equation (2), estimated from

Table 3 Magnetic parameters derived from curve fitting of the temperature dependence of molar susceptibility data for diruthenium derivatives

Compound	g	$-J$/cm^{-1}	$10^6 N_\alpha$/ cm^3 mol^{-1}
1	2.3	728	196
2	2.3	649	184
6 Na[Ru_2(dhpta)(μ-$O_2CMe)_2$]*	2.4	470	263
7 Na[Ru_2(dhpta)(μ-$O_2CPh)_2$]*	2.0	310	180

* From ref. 9.

Table 4 Electrochemical data for diruthenium derivatives in dmf[a]

	$E_{\frac{1}{2}}$/V				
Compound	1	2	3	$\Delta E^{1,2}$/V	K_c
1	−1.80	−1.23	0.73	0.57	4.4×10^9
2	−1.74	−1.13	0.81	0.61	2.1×10^{10}
3	−1.74	−1.15	0.79	0.59	9.6×10^9
4	−1.78	−1.18	0.76	0.60	1.4×10^{10}
6 Na[Ru_2(dhpta)-(μ-$O_2CMe)_2$][b]	−1.81	−1.28	0.57	0.53	9.1×10^8
7 Na[Ru_2(dhpta)-(μ-$O_2CPh)_2$][b]	−1.64	−1.24	0.59	0.40	5.8×10^6

[a] *vs.* Ag–$AgPF_6$. [b] From ref. 9.

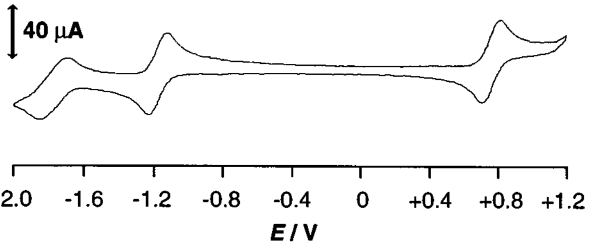

Fig. 4 Cyclic voltammogram for K[$Ru_2L(\mu\text{-}O_2CPh)_2$] **4** in 1 mM dmf solution with 0.1 M [NBu^n_4][PF_6] as supporting electrolyte. Potentials were referenced to Ag–$AgPF_6$

$$[Ru^{II}Ru^{II}L(O_2CR)_2]^{3-} + [Ru^{III}Ru^{III}L(O_2CR)_2]^{-} \overset{K_C}{\rightleftharpoons} 2[Ru^{II}Ru^{III}L(O_2CR)_2]^{2-} \quad (2)$$

the redox potential gap between the two reduction processes ($\Delta E^{1,2} = |E^1_{\frac{1}{2}} - E^2_{\frac{1}{2}}|$) for L complexes as depicted in equation (3),

$$K_C = \exp\left(\frac{\Delta E^{1,2} n_1 n_2 F}{RT}\right) \quad (3)$$

where n_1 and n_2 are the number of electrons being transferred in the redox processes E^1 and E^2, are also listed in Table 4. The values are remarkably larger than those for the corresponding dhpta complex, indicating that the $Ru^{II}Ru^{III}$ mixed-valence state could be fairly stabilized by the aryloxo-bridged structure. The electron withdrawing nature of the phenolate oxygen promotes the one-electron reduction of Ru^{III}_2 species generating mixed-valence complexes, whereas intervalence stabilization between two metal centres resists further one-electron reduction resulting in rather negative second reduction potentials ($E^1_{\frac{1}{2}}$).

Conclusion

To explore novel functions of diruthenium cores, the present work has been carried out by utilizing ligand L and modifying the monoatom bridge from a μ-alkoxo to a μ-aryloxo group. The (μ-aryloxo)bis(μ-carboxylato)diruthenium(III) complexes M[$Ru_2L(\mu\text{-}O_2CR)_2$] **1**–**4** (M = Na or K, R = Me or Ph) were successfully prepared and characterized, revealing that their magnetic and electrochemical properties can be altered by varying the monoatom bridging group. Meaningfully large antiferromagnetic spin coupling constants ($-J = 728$ and 649 cm^{-1} for **1** and **2**, respectively) and intervalence coupling constants for the Ru^{II}–Ru^{III} couple ($K_C = 4.4 \times 10^9$–2.1×10^{10}) were obtained. The μ-aryloxo group increases the metal–metal electronic interaction through its p orbitals without any dramatic structural changes: single-crystal X-ray crystallography of **4** revealed that the Ru···Ru distance is preserved at around 3.4 Å.

Acknowledgements

This work was partially supported by a Grant-in-Aid for Scientific Research from the Ministry of Education, Science, Sports and Culture 10131247 and 10894022, and grants from Nippon Itagarasu and Rigaku-Denki and the San-Ei Gen Foundation. The authors thank Professor Kotaro Osakada of the Tokyo Institute of Technology, Professor Yuzo Nishida of Yamagata University, Professor Masaaki Haga of Mie University and Yoichi Sasaki of Hokkaido University for their helpful suggestions.

References

1 S. J. Lippard, *Angew. Chem., Int. Ed. Engl.*, 1988, **27**, 344.
2 D. M. Kurtz, jun., *Chem. Rev.*, 1990, **90**, 585.
3 A. Feig and S. J. Lippard, *Chem. Rev.*, 1994, **94**, 759.
4 P. Neubold, K. Wieghardt, B. Nuber and J. Weiss, *Inorg. Chem.*, 1989, **28**, 459.
5 P. Neubold, B. S. P. C. Della Vedva, K. Wieghardt, B. Nuber and J. Weiss, *Inorg. Chem.*, 1990, **29**, 3355.
6 B. K. Das and A. R. Chakravarty, *Inorg. Chem.*, 1991, **30**, 4978.
7 C. Sudha, S. K. Mandal and A. R. Chakravarty, *Inorg. Chem.*, 1993, **32**, 3801.
8 T. Tanase, M. Kato, Y. Yamada, K. Tanaka, K. Lee, Y. Sugihara, A. Ichimura, I. Kinoshita, M. Haga, Y. Sasaki, Y. Yamamoto, T. Nagano and S. Yano, *Chem. Lett.*, 1994, 1853.
9 T. Tanase, Y. Yamada, K. Tanaka, T. Miyazu, M. Kato, K. Lee, Y. Sugihara, W. Mori, A. Ichimura, I. Kinoshita, Y. Yamamoto, M. Haga, Y. Sasaki and S. Yano, *Inorg. Chem.*, 1996, **35**, 6230.
10 B. P. Murch, F. C. Bradley, P. D. Boyle, V. Papaefthmiou and L. Que, jun., *J. Am. Chem. Soc.*, 1987, **109**, 7993.
11 G. M. Sheldrick, in *Crystallography Computing*, eds. G. M. Sheldrick, C. Kruger and R. Goddard, Oxford University Press, Oxford, 1985, p. 175.
12 D. T. Cromer and J. T. Weber, *International Tables for X-Ray Crystallography*, Kynoch Press, Birmingham, 1974, vol. 4.
13 D. C. Creagh and W. J. McAuley, *International Tables for Crystallography*, Kluwer, Boston, 1992, vol. C.
14 TEXSAN, Molecular Structure Corporation, The Woodlands, TX, 1985 and 1992.
15 C. K. Johnson, ORTEP II, Report ORNL-5138, Oak Ridge National Laboratory, Oak Ridge, TN, 1976.

Received 2nd *February* 1998; *Paper* 8/00857D